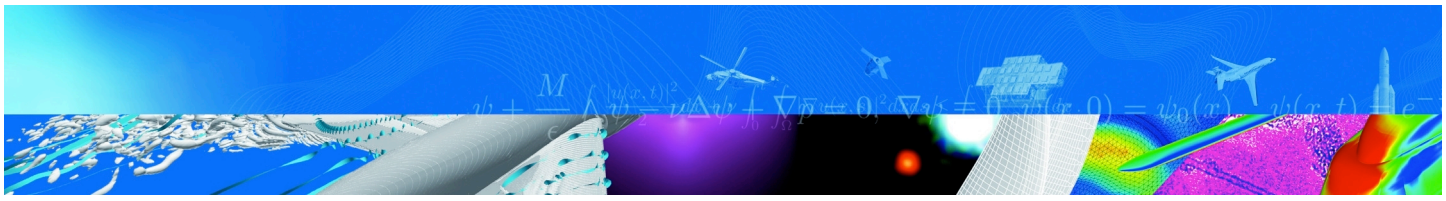

ONERA

THE FRENCH AEROSPACE LAB

return on innovation

PROGRESS REPORT

Convex design of a Youla parameter for LTI and LFT plant models

Author: G. FERRERES

SYSTEMS CONTROL
AND FLIGHT DYNAMICS DEPARTMENT

IR 1/19678 DCSD - March, 2014

UNCLASSIFIED

ONERA

THE FRENCH AEROSPACE LAB

Toulouse Center
B.P. 74025 - 2, Avenue E. Belin
F-31055 TOULOUSE CEDEX 4
Phone (33) 5.62.25.25.25 - Fax 5.62.25.25.64
http://www.onera.fr/dcsd/
French National Aerospace Research Establishment

DÉPARTEMENT

SYSTEMS CONTROL AND FLIGHT DYNAMICS

Intermediate Report IR 1/19678 DCSD

Convex design of a Youla parameter for LTI and LFT plant models

March, 2014

Author

G. FERRERES

Checked by :
G. FERRERES

Approved by :
F. JOUHAUD
Interim Head of Systems Control
and Flight Dynamics Department

DCSD-T n^{r} c 26/2014

UNCLASSIFIED

UNCLASSIFIED

IDENTIFICATION SHEET of ONERA document # IR 1/19678 DCSD

Issuing department:	Contracting party:	Contract references:
Systems Control and Flight Dynamics		
	Program record # :	Date: March, 2014
Title: *Convex design of a Youla parameter for LTI and LFT plant models*		
Author: G. FERRERES		

PROTECTION Level:		PROTECTION Release:	
Title	: Unclassified	Title	: not applicable
Sheet	: Unclassified	Sheet	: not applicable
Document	: Unclassified	Document	: not applicable

Author abstract

A feedback controller design technique is presented, which accounts for time- and frequency-domain closed loop specifications. A convex optimization problem is to be solved, whose constraints and minimization objectives directly correspond to these spec. This allows to study the feasibility of a set of design specifications, and more generally to explore the trade-off between these specifications. An LTI closed loop is considered first, before a gain-scheduled one under an LFT form. Applications to an LTI flexible aircraft model and to an LFT missile model are presented.

Keywords

LFT

Toulouse Center
B.P. 74025 - 2, Avenue E. Belin
F-31055 TOULOUSE CEDEX 4
Phone (33) 5.62.25.25.25 - Fax 5.62.25.25.64
http://www.onera.fr/dcsd/
French National Aerospace Research Establishment

ONERA
THE FRENCH AEROSPACE LAB

UNCLASSIFIED

DISTRIBUTION LIST of ONERA document # IR 1/19678 DCSD

Document only

- *Outside ONERA*
- *Inside ONERA*

  DCT/CID ..... 1 ex.
  Interim Head DCSD : F. JOUHAUD ..... 1 ex.

  Adjoint(s) de Gestion ..... 1 ex.

  Diffusion intranet ONERA

Identification sheet only

- *Outside ONERA*
- *Inside ONERA*
  PH. BIDAUD (DSB/TIS) - CID Toulouse
- *Systematic distribution*
  No distribution
- *Electronic distribution*
  No distribution

Toulouse Center
B.P. 74025 - 2, Avenue E. Belin
F-31055 TOULOUSE CEDEX 4
Phone (33) 5.62.25.25.25 - Fax 5.62.25.25.64
http://www.onera.fr/dcsd/
French National Aerospace Research Establishment

ONERA
THE FRENCH AEROSPACE LAB

Contents

Chapter 1

Introduction

As a main drawback for practitioners, many control design techniques account for a given set of design specifications only in an indirect way, so that it often appears difficult to satisfy them without a large amount of tuning. It appears even more difficult to check their feasibility, and more generally to explore the necessary trade-offs between these specifications, especially when a non-convex optimization problem is to be solved: nothing can be concluded if the solver does not succeed in satisfying the constraints, i.e. the design specifications, since only a local optimum is obtained. The global optimum may satisfy them, or not.

In this context, a two-step solution was proposed in [6] for the control of an LTI model. The first step is to build a Youla parameterization of *all* stabilizing controllers, on the basis of on initial stabilizing controller possibly under an observed state feedback form [4, 5, 17, 12, 2]. Next, a Youla parameter $Q(s)$ is computed so as to satisfy the design specifications. Last, the feedback controller is deduced as a combination of the initial stabilizing controller and of the optimized $Q(s)$.

As a crucial point, computing the Youla parameter reduces to a convex optimization problem, where the minimization objective and constraints directly correspond to the closed loop time- or frequency-domain design specifications. Since the whole set of stabilizing controllers is handled, this enables to check their feasibility, and more generally to explore the necessary trade-offs between these specifications. See e.g. [11] for an application to a flexible aircraft model.

Extending this valuable method to the gain-scheduled and nonlinear cases needs to solve two different problems:

- Extending the Youla-parameterization technique: see e.g. [14, 3, 9] for the case of a nonlinear or gain-scheduled plant, possibly under an LFT form. The main point is to determine if the whole set of stabilizing controllers is obtained.

- Designing the Youla parameter: when the issue is to satisfy LTI design specifications on a set of LTI models corresponding to a continuum of trim points

or to a trajectory of the nonlinear plant, to a large extent the problem can be reduced to a convex optimization problem, as in the original LTI case. This is (much) less obvious in the other cases, especially in the case of a fully nonlinear plant.

The report is organized as follows:

- Chapter 2 presents the technique for the case of an LTI model. Youla parameterization is explained first, before discussing how to design the initial controller. A cutting planes frequency-domain solver is also presented, for the convex design of a Youla parameter satisfying time-and frequency-domain specifications. This solver is especially suited to the case of high order models, for which state-space solutions [21, 24] cannot be applied.

- Chapter 3 presents an application to the lateral control of a flexible aircraft, extracted (and modified) from [8, 11]. The initial observed state feedback controller can be designed using a LQ/modal technique, or a loop shaping H_∞ technique [17, 12]. The Youla parameter is computed with the cutting planes solver, and the trade-off between the two design specifications is studied.

- Chapter 4 presents an extension of the technique to the LFT case [9], with an application to a missile example extracted from [19] in chapter 5. One focuses on the case of an LFT model describing LTI models corresponding to a continuum of trim points, parameterized as a function of time invariant scheduling parameters. Thus, the design specifications are to be satisfied on the continuum of LTI models. The initial observed state feedback LFT controller is designed using a (multi-model) polytopic technique [7] extended to the gain-scheduled case, and validated with a μ analysis technique [8, 10]. In the same way, the Youla parameter is designed on a gridding of models, and this multi-model design is validated on the continuum using μ analysis.

Chapter 2

Convex design of a Youla parameter for an LTI plant model

2.1 Youla parameterization

2.1.1 Principle

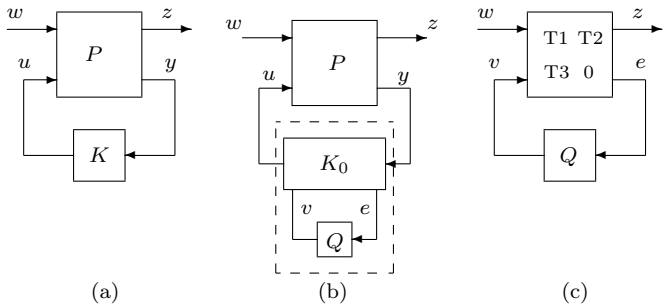

Figure 2.1: The design problem (a) and Youla parameterization (b,c).

Consider the standard design problem of figure 2.1.a, where $P = \begin{bmatrix} P_{11} & P_{12} \\ P_{21} & P_{22} \end{bmatrix}$ is an augmented plant. The closed loop transfer matrix $F_l(P, K) = P_{11} + P_{12}K(I - P_{22}K)^{-1}P_{21}$ is a highly nonlinear function of controller K, especially because of the need to invert $I - P_{22}K$. Suppose an initial stabilizing controller K_0, whose order is at least equal to the order of P_{22}, is available. Additional inputs and outputs v and e are introduced in K_0 (see figure 2.1.b), with the key constraint that the transfer matrix between v and e is zero: see figure 2.1.c. A solution to achieve this property is to put K_0 under the form of an observed state feedback controller [4, 5, 2], see also below. Then, when connecting a free stable transfer matrix Q to these additional inputs and outputs, $F_l(P, K)$ can be rewritten as $T_1 + T_2QT_3$, where fixed transfer

matrices T_i depend on P and K_0, while Q is the design parameter.

The parameterization $T_1+T_2QT_3$ covers the whole set of achievable closed loops: given any stabilizing feedback controller K, there exists a corresponding value of the stable Youla parameter Q that gives the same closed loop (i.e. $F_l(P,K) = T_1 + T_2QT_3$), and conversely. As a consequence let $Q = \sum_i \theta_i Q_i$, where filters Q_i are fixed while the θ_i are the design parameters. If the infinite dimensional basis of filters Q_i covers the whole set of stable transfer matrices, the whole set of stabilizing feedback controllers K is described. Thus, it becomes possible to check whether there exists a controller, whose order is free, that satisfies a set of design specifications.

Summarizing, given a standard design problem, see figure 2.1.a, there are 5 steps in practice:

1. Computation of the initial controller $K_0(s)$.
2. Computation of the Youla parameterization $T_1(s) + T_2(s)Q(s)T_3(s)$.
3. Choice of a finite-dimensional basis of filters $Q(s) = \sum_{i=1}^{n} \theta_i Q_i(s)$, i.e. choice of the filters $Q_i(s)$.
4. Convex design of the Youla parameter $Q(s)$ by optimizing w.r.t. the parameters θ_i, so as to satisfy a set of time- and frequency domain specifications.
5. Computation of the feedback controller $K(s)$ as the interconnection of $K_0(s)$ and $Q(s)$, see figure 2.1.b.

2.1.2 The case of an observed state feedback controller

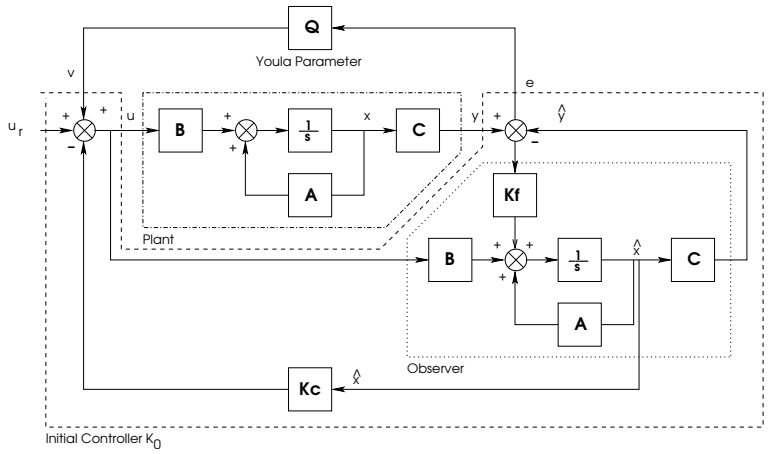

Figure 2.2: Youla parameterization with an observed state feedback controller.

Figure 2.2 presents the architecture of the controller, when using an observed state feedback controller (or a controller that was put under such form) as the initial one for Youla parameterization. e is now the prediction error, while v is an additive disturbance on the control input u. Assume that $x = \hat{x}$ at $t = 0$ and that the open loop plant model, which is embedded inside the observer, exactly coincides with the "true" open loop plant. Despite a non-zero input v the prediction error e stays identically zero, since the observer accounts for the measured disturbance v. Thus, the transfer function between v and e is zero, as required.

In the same way, the transfer function between $u_r = H(s)y_r$ and e is zero, which means that a non-zero reference input y_r, introduced with a feedforward controller $H(s)$, just excites the closed loop state feedback dynamics, not the observer one nor the dynamics of $Q(s)$, at least in the absence of model uncertainties.

2.1.3 Choice of the basis of filters

For the ease of presentation, only the SISO case is considered. When choosing a basis of filters the main point is to choose its dynamics, i.e. its poles. As a first simple example, if a real pole $-a$ and a complex pole with frequency ω and damping ratio ξ are considered, a basis of 4 filters is obtained as:

$$Q(s) = \theta_1 + \frac{\theta_2}{s+a} + \frac{\theta_3}{s^2 + 2\xi\omega s + \omega^2} + \frac{\theta_4 s}{s^2 + 2\xi\omega s + \omega^2} \tag{2.1}$$

Nevertheless, to improve the numerical conditioning of the convex optimization problem which will be to be solved, it is much better using an orthonormal basis of filters. In the following, the basis of [1] will be used:

$$Q_i(s) = \frac{\sqrt{2Re(a_i)}}{s+a_i} \Pi_{k=1}^{i-1} \frac{s - \overline{a}_k}{s + a_k} \tag{2.2}$$

Here again, the issue is to choose the real or complex conjugate poles $-a_i$ on the basis of our physical knowledge of the open- or closed-loop plant. As an additional advantage of using an orthonormal basis instead of (2.1), it is possible to guarantee that the whole set of asymptotically stable $Q(s)$ is recovered when using the infinite dimensional basis (2.2), under a condition on its poles.

Last note that the basis of [1] includes the special case of Laguerre (Kautz) basis, which is recovered by choosing for all $-a_i$ the same real pole (the same pair of complex conjugate poles). But the interest of [1] is to be able to introduce different dynamics in the same basis, so that if the choice of the poles $-a_i$ is adequate, less filters are needed to cover the same part of the whole set of asymptotically stable transfer matrices. Thus, the computational burden is reduced.

2.2 A cutting planes method for time- and frequency-domain specifications

Generally speaking, a norm constraint on the closed loop transfer matrix $T_1+T_2QT_3$ is convex with respect to $Q = \sum_i \theta_i Q_i$. As a consequence, when constraining or minimizing the norm of various parts of the closed loop transfer matrix $T_1 + T_2QT_3$, a convex optimization problem with convex constraints is obtained. Optimal values of the design parameters θ_i are computed, $Q(s)$ is deduced as well as $K(s)$ (see figure 2.1.b).

A state-space LMI solution can be found in [21, 24]: let (A_Q, B_Q, C_Q, D_Q) be a state-space representation of $Q(s)$. A_Q and B_Q are supposed to be fixed in [21], while the optimization matrix is $N = [C_Q \ D_Q]$. If $Q(s) = \sum_{i=1}^{N} \theta_i Q_i(s)$, a state-space representation of $Q(s)$ can be found where the optimization parameters θ_i are gathered in C_Q and D_Q.

Nevertheless, this LMI method becomes untractable when the order of the state-space model becomes too high, which is especially the case of a flexible aircraft model [11]. As a consequence, a cutting planes method is proposed in the following, which deals with the special case of time- and frequency-domain constraints. A case which is often encountered in practice.

2.2.1 Time-domain specifications

Let:

$$z(t) = T(s,\theta)w(t) = \left(T_1(s) + T_2(s)(\sum_i \theta_i Q_i(s))T_3(s)\right) w(t)$$

Assume that the unmeasured disturbance signal $w(t)$ is fixed (e.g. a step). Noting $z_0(t) = T_1(s)w(t)$ and $z_i(t) = T_2(s)Q_i(s)T_3(s)w(t)$, on obtains $z(t) = z_0(t) + \sum_i \theta_i z_i(t)$. As a consequence, in the context of e.g. a step response, minimizing the overshoot is equivalent to minimize the scalar optimization parameter γ under the constraint:

$$z_0(t) + \sum_i \theta_i z_i(t) \leq \gamma \ \ \forall t$$

In the same way, a constraint on the settling time can be written as:

$$0.9 \leq z_0(t) + \sum_i \theta_i z_i(t) \leq 1.1 \ \ \forall t \geq T$$

Generally speaking, when stacking the time-domain specifications, an LP problem $A\theta \leq b$ is obtained, or possibly $A \begin{bmatrix} \theta \\ \gamma \end{bmatrix} \leq b$, where γ is to be minimized.

2.2.2 Frequency-domain specifications

Here again, let $T(s,\theta) = T_1(s)+T_2(s)(\sum_i \theta_i Q_i(s))T_3(s)$, and let $\alpha(\omega)$ be a frequency-domain template. The H_∞ constraint over a finite frequency interval:

$$\overline{\sigma}\left(T(j\omega,\theta)\right) \leq \alpha(\omega)\ \forall \omega \in [\omega_1,\ \omega_2]$$

is convex w.r.t. the optimization parameters θ_i, because of the affinity of the closed loop transfer matrix $T(s,\theta)$ w.r.t. θ.

Analogously, an H_∞ minimisation objective corresponds to the minimisation of γ under the convex constraint:

$$\overline{\sigma}\left(T(j\omega,\theta)\right) \leq \gamma\ \alpha(\omega)\ \forall \omega \in [\omega_1,\ \omega_2] \tag{2.3}$$

In the same spirit, one can consider either a convex constraint on the extended H_2 norm of the transfer matrix $T(s,\theta)$ on a finite frequency interval:

$$\sqrt{\frac{1}{2\pi}\int_{\omega_3}^{\omega_4} Trace(T^*(j\omega,\theta)T(j\omega,\theta))d\omega} \leq C \tag{2.4}$$

where C is a constant, or the convex minimization of this extended H_2 norm. In both cases, the square of the H_2 norm in (2.4) can be approximated as a quadratic criterion $f_0 + f^T\theta + \theta^T Q\theta$ using a fine enough frequency gridding.

2.2.3 Principle of the frequency-domain cutting planes method

Wu just explain the principle of this classical method. The idea is to approximate the *non-differentiable* convex constraint (2.3) at $\theta = \theta^0$ by an affine one:

$$\overline{\sigma}(T(j\omega,\theta^0)) + S^T(\theta-\theta^0) \ \ \leq \ \ \gamma\ \alpha(\omega) \tag{2.5}$$

where S is called a subgradient. Indeed, for all θ:

$$\overline{\sigma}(T(j\omega,\theta^0)) + S^T(\theta-\theta^0) \ \ \leq \ \ \overline{\sigma}(T(j\omega,\theta))$$

When approximating (2.3) at differents points $\theta = \theta^i$ and at different frequencies $\omega = \omega_i$, all these affine constraints (2.5) can be stacked into an LP constraint $A\begin{bmatrix}\theta\\ \gamma\end{bmatrix} \leq b$. More generally, when considering the minimization of a convex objective under convex constraints, a lower bound of the minimal value γ^* of the objective is computed as the minimal value of γ under the LP constraints above. The idea is to refine this affine approximation of the convex optimization problem until γ^* is computed with a satisfactory accuracy, as illustrated by the following sketch of algorithm:

1. Compute the value $\tilde{\theta}$ of θ that minimizes γ under the LP constraints. Let γ_{lb} be the associated minimal value of γ.

2. Compute an upper bound γ_{ub} of γ^*, noting that any value of θ satisfying the constraints provides an upper bound. If the gap between the bounds is close enough STOP. Otherwise approximate convex constraints and minimization objectives at $\theta = \tilde{\theta}$ and at critical frequencies, where constraints are the most violated. Return to step 1.

Remark: more precisely, as illustrated in chapter 3, the above algorithm is performed for a given design frequency gridding, i.e. the specifications are to be satisfied on this gridding at the end of the algorithm. Next, the result, i.e. the optimal value of $Q(s)$, is validated on a (much) finer frequency gridding. If the specifications are satisfied on this validation gridding, STOP. Otherwise, determine the critical frequencies, where constraints are the most violated, add them to the design frequency gridding, and perform the above algorithm on this new gridding.

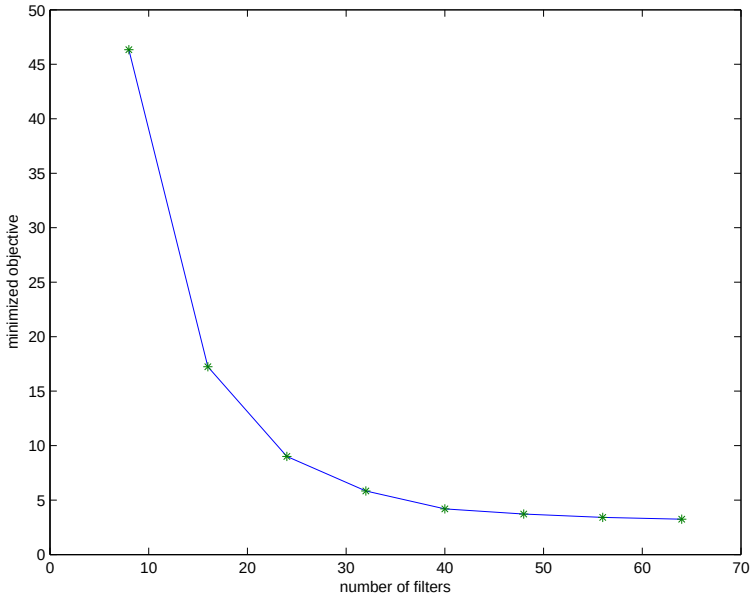

Figure 2.3: Minimized value of the objective as a function of the number of used filters $Q_i(s)$.

The use of a cutting planes method makes possible a progressive convex design in the case of a large number of optimization parameters θ_i. If there are e.g. 64 optimization parameters, only the first 8 optimization parameters are first used, and the associated value of the minimized objective is computed. Then the first 16 optimization parameters are used, and the value of the minimized objective is computed here again. Until all 64 optimization parameters are used. The decrease

of the minimized objective is visualized as a function of the number of optimization parameters: see the example of figure 2.3, extracted from next chapter. If the value of the minimized objective tends towards an asymptotic value, this means that adding more filters is useless, i.e. the value of the minimized objective, corresponding to an infinite dimensional basis of filters, is obtained.

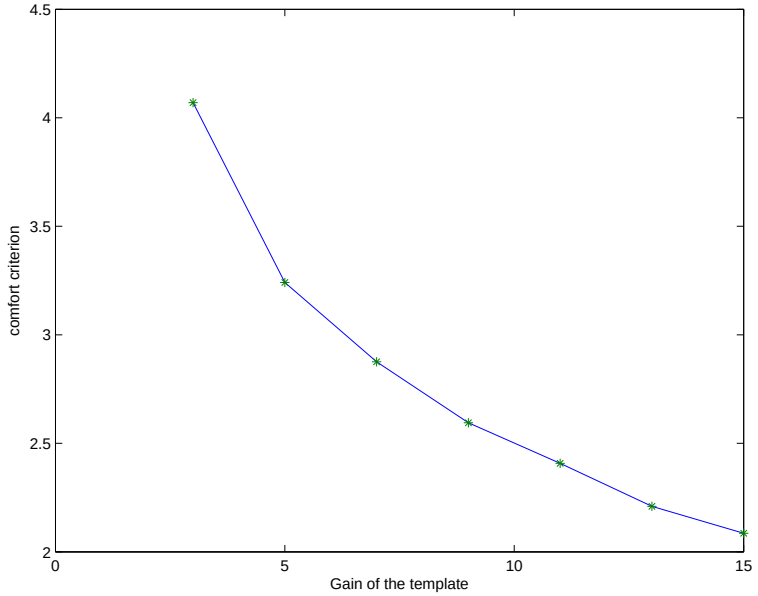

Figure 2.4: Minimized value of the objective as a function of actuator activity.

During this progressive design subgradients are kept from an optimization to an other in order to save a large amount of computational time. In the same way, it is possible to study the trade-offs between the design specifications. The issue is to minimize an objective under several constraints, where one of these constraints takes several values. Depending on the hardness of this constraint it is more or less possible to minimize the objective: see the example of figure 2.4, extracted from next chapter, where the x-axis (more or less) represents actuator activity while the y-axis represents the minimized objective. The lower the allowed actuator activity, the harder the constraint, the higher the minimized objective. Here again it is possible to save a large amount of computational time by keeping subgradients from an optimization to an other.

2.3 Design of an initial controller

2.3.1 Modal design of an observed state feedback controller

Let $(A, B, C, 0)$ be a state-space representation of the open loop plant model. The issue is to design K and L, which place the eigenvalues of $A - BK$ and $A - LC$. A first solution exactly places all closed loop poles at given locations, which is possible in the special cases of state feedback and observer gains. Nevertheless, it is necessary to choose these eigenvalues, and also the associated eigenvectors if there is more than one input or output.

A much simpler "minimum energy" solution uses LQ control. Let K be the optimal state feedback controller associated to the weights $Q = 0$ and $R = I$, for a plant model $\dot{x} = Ax + Bu$. If the plant is asymptotically stable, $K = 0$ is obtained. Otherwise, if there is an "unstable" pole $x + jy$, with $x > 0$, the state feedback controller moves it to $-x + jy$ ("mirror effect"). Even if the open loop plant model is asymptotically stable, when using $(A + \lambda I, B)$ as the plant model with $\lambda > 0$, poles can be moved if their real part is greater than $-\lambda$.

Obviously, this technique does not enable a fine placement of the closed loop poles, since the only tuning parameter is λ. But this very simple method can be used to design an initial controller which may satisfy, at least partly, the design specifications: see section 3.2.

Last note that the method is easily extended to the case of an observer gain, by applying the LQ control technique to the plant model $(A^T + \lambda I, C^T)$.

2.3.2 Loop shaping H_∞ control

Principle

Classical H_∞ control shapes closed loop transfer matrices, whereas loop shaping H_∞ control shapes the open loop. Let $G(s)$ be the plant model. Pre- and post-compensators $W_1(s)$ and $W_2(s)$ are determined, so that the ideal open loop is $G_s(s) = W_2(s)G(s)W_1(s)$. The issue is to preserve this open loop shape as much as possible. To this aim loop shaping H_∞ control synthesizes a controller $K_\infty(s)$, that stabilizes G_s while maximizing the robustness to neglected dynamics on the coprime factors of G_s. A direct solution to this specific H_∞ problem, without γ iterations, is available, as well as a natural observed-state feedback form for $K_\infty(s)$ [17, 12]. The final controller is $W_1(s)K_\infty(s)W_2(s)$.

In practice, the main issue is to choose the pre- and post-compensators $W_1(s)$ and $W_2(s)$. In the context of the design of an initial controller for Youla parameterization, these compensators should be chosen as simple as possible, as illustrated in section 3.2.

Numerical computation

Let $(A, B, C, 0)$ be a state-space model of $W_2(s)G(s)W_1(s)$, noting that a non strictly proper model could be handled. The issue is to solve the two Riccati equations:

$$A'X + XA - XBB'X + C'C = 0 \quad (2.6)$$
$$AZ + ZA' - ZC'CZ + BB' = 0 \quad (2.7)$$

The minimal value of the H_∞ norm is obtained as:

$$\gamma_{min} = \sqrt{1 + \lambda_{max}(XZ)} \quad (2.8)$$

In practice, γ is chosen slightly higher than γ_{min}. The controller $K_\infty(s)$ has the observed state feedback form:

$$\dot{\hat{x}} = (A - LC - BK)\hat{x} + Ly + Bu_r \quad (2.9)$$
$$u = -K\hat{x} + u_r \quad (2.10)$$

u and y are the I/O of the open loop model, namely $W_2(s)G(s)W_1(s)$, u_r is a reference input and the state feedback and observer gains K and L are computed as:

$$L = ZC' \quad (2.11)$$
$$K = -\gamma^2 B'XW_1^{-T} \quad (2.12)$$
$$W_1 = I + XZ - \gamma^2 I \quad (2.13)$$

A last issue is to deduce an observed state feedback controller for $G(s)$, since the controller $K_\infty(s)$ above is applied to $W_2(s)G(s)W_1(s)$. In other words, one would like to obtain an observed state feedback form for the true feedback controller $W_1(s)K_\infty(s)W_2(s)$. Following [11] and the next applicative chapter, one just considers the following special case. If $W_2(s)G(s)W_1(s) = S\ G(s)\ K_{ref}$, then the observed state feedback controller is:

$$\dot{\hat{x}} = (A - LSC - BK_{ref}K)\hat{x} + LSy + Bu_r \quad (2.14)$$
$$u = -K_{ref}K\hat{x} + u_r \quad (2.15)$$

EMPTY PAGE

Chapter 3

A flexible aircraft application

3.1 Problem description

The issue is to design a lateral flight control system, whose structure is given on figure 2.2, for a flexible transport aircraft. The model, whose order is 21 with 2 inputs (aileron and rudder deflections) and 4 outputs ny, p, r, ϕ, contains 4 rigid states (the sideslip angle β, the rotational rates p and r, and the bank angle ϕ), 12 flexible states corresponding to 6 bending modes, and 5 actuators states [8].

The design specifications are the following. Consider the interconnection of the aircraft model with the controller $K(s)$. Let z denote the controller output. An additive unmeasured disturbance input w is added at the plant input. Since there are 2 plant inputs, the dimension of w and z is 2. When introducing a block of neglected dynamics between w and z, this block corresponds to an unstructured direct additive model perturbation at the plant input, representative of unmodeled high frequency bending modes.

Let $M_1(s)$ (resp. $M_2(s)$) be the closed loop SISO transfer function between the disturbance w_1 (resp. w_2) on the first (resp. second) aircraft input and the acceleration ny. Let $M_3(s)$ be the closed loop MIMO transfer matrix between w and z. The issue is to minimize α under the constraints (for ω between 5 and 25 rad/s):

$$\begin{aligned} |M_1(j\omega)| &\leq \alpha \\ |M_2(j\omega)| &\leq \alpha \end{aligned}$$

and under the additional constraint (for ω between 0 and 1000 rad/s):

$$\overline{\sigma}(M_3(j\omega)) \leq |F(j\omega)| \tag{3.1}$$

where:

$$F(s) = \frac{G}{(1 + 1.4\frac{s}{\omega_0} + \frac{s^2}{\omega_0^2})(1 + \frac{s}{\omega_0})}$$

The choice of the tuning parameters G and ω_0 will be discussed later.

The issue is to globally minimize the frequency-domain peaks on output ny, due to flexible modes (whose effect is roughly between 5 and 25 rad/s), under a double constraint:

1. on the actuator activity: this corresponds to the constraint (3.1) at low and middle frequencies, and thus, to some extent, to the tuning parameter G.

2. on the roll-off, and thus on the robustness to unmodeled high frequency bending modes: this corresponds to the constraint (3.1) at high frequencies, and thus, to some extent, to the tuning parameter ω_0.

Remark: if $K(s) = 0$, $M_1(s)$ (resp. $M_2(s)$) corresponds to the open loop SISO transfer function between the first (resp. second) aircraft input and ny, so that the effect of the feedback controller on the frequency-domain peaks can be directly evaluated.

3.2 Design of the initial controller

The methods of sections 2.3.1 and 2.3.2 are tested. The issue is to determine to which extent each method is able to provide an initial controller satisfying (part of) the design specifications. One focuses on the minimization of the frequency-domain peaks on output ny.

The modal / LQ control design technique is tested first, with $\lambda = 1$. Figure 3.1 (resp. 3.2) presents the open loop transfer function between the first (resp. second) plant input and output ny, as well as the closed loop transfer function between w_1 (resp. w_2) and ny. The peaks due to flexible modes are reduced to some extent.

The loop shaping H_∞ design technique is considered next. Let $G(s)$ be the open loop aircraft model with 2 inputs (aileron and rudder deflections) and 4 outputs ny, p, r, ϕ. A willingly very simple choice for the pre- and post-compensators is $W_1(s) = I$ and $W_2(s) = diag(w, 1, 1, 1)$, i.e. the augmented open loop plant is $diag(w, 1, 1, 1)\ G(s)$, where the weight w on the output ny is chosen as $w = 20$.

Figure 3.3 (resp. 3.4) presents the open loop transfer function between the first (resp. second) plant input and output ny, as well as the closed loop transfer function between w_1 (resp. w_2) and ny. Here again, the peaks due to flexible modes are reduced to some extent.

As a conclusion, peaks can be reduced with the 2 methods, and the reduction ratio depends on one tuning parameter. Nevertheless, an advantage of loop shaping H_∞ control is to directly account for I/O specifications, so that this method is chosen in the following to design the initial controller.

Remark: a more sophisticated use of these techniques would be required to account for handling qualities [11], i.e. the specifications on the rigid part of the aircraft.

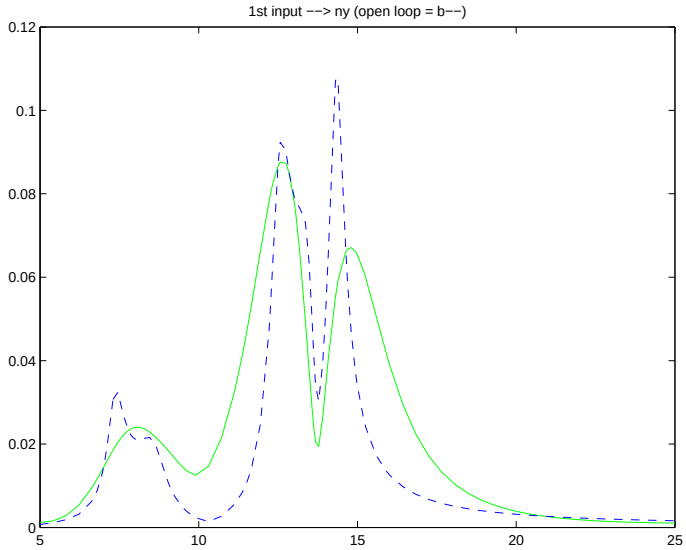

Figure 3.1: Open (dashed line) and closed (solid line) loop frequency response to the first input with the observed state feedback controller.

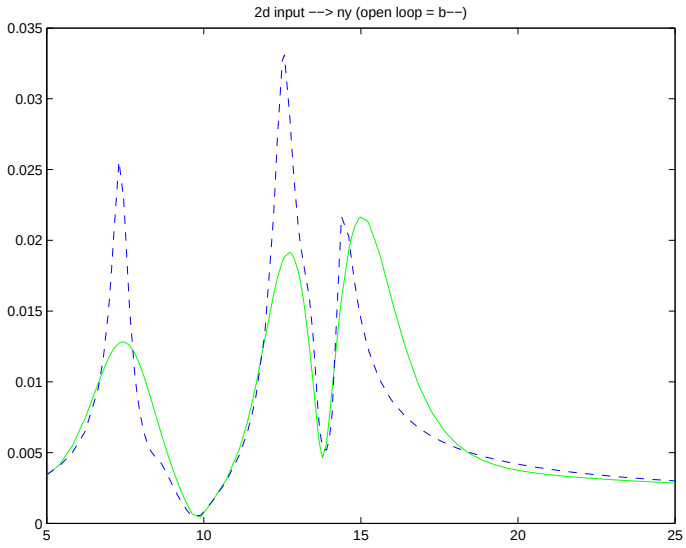

Figure 3.2: Open (dashed line) and closed (solid line) loop frequency response to the second input with the observed state feedback controller.

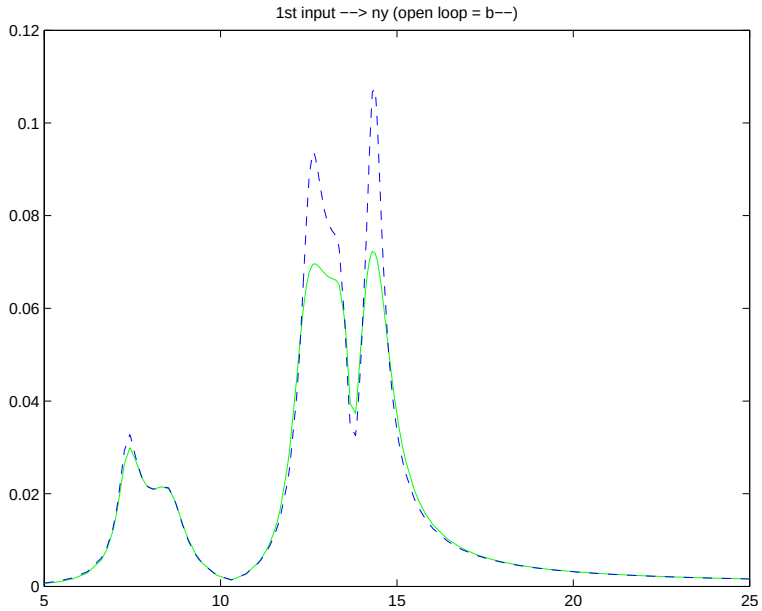

Figure 3.3: Open (dashed line) and closed (solid line) loop frequency response to the first input with the loop shaping H_∞ controller.

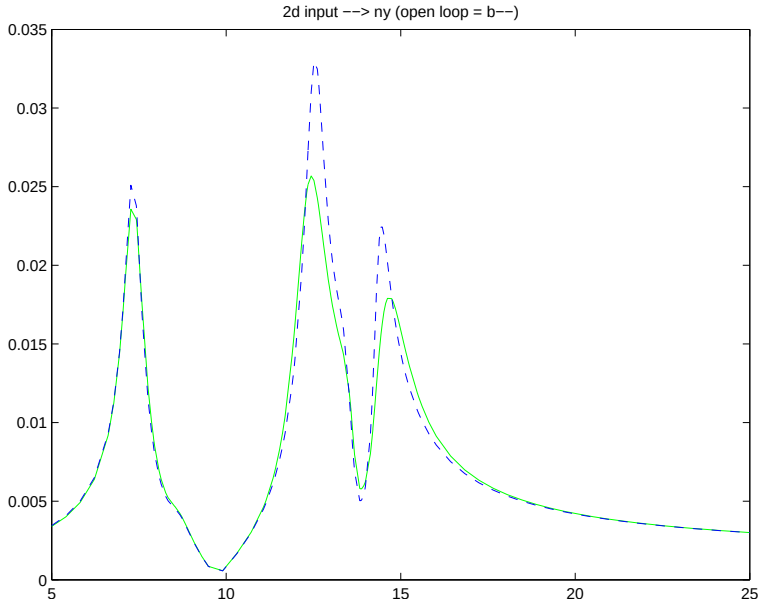

Figure 3.4: Open (dashed line) and closed (solid line) loop frequency response to the second input with the loop shaping H_∞ controller.

3.3 Design of the Youla parameter and computation of design tradeoffs

The basis of [1] is used with the following poles, whose damping ratio is 0.7 and whose frequency is chosen between 5 and 25 rad/s:

$$5\frac{-1\pm j}{\sqrt{2}}\ \ 8\frac{-1\pm j}{\sqrt{2}}\ \ 12\frac{-1\pm j}{\sqrt{2}}\ \ 15\frac{-1\pm j}{\sqrt{2}} \tag{3.2}$$

Since $Q(s)$ has 2 outputs and 4 inputs this corresponds to 64 filters. Following section 3.1, two H_∞ objectives are minimized under an H_∞ constraint, with tuning parameters $\omega_0 = 20\ rad/s$ and $G = 5$.

A progressive design is performed with 8, 16,. . . , 64 filters. An asymptotic value for the minimized objective $\alpha \approx 3.3$ is obtained on figure 2.3, which suggests that the value α of the minimized objective, corresponding to an infinite dimensional basis of filters, is obtained. The computational time is 59 s, which is very reasonable when considering the complexity of this high dimensional problem. The H_∞ constraint is displayed on figures 3.5 and 3.6 for the initial and optimal controllers: as expected, the constraint is (highly) active after optimization.

Remarks:
(*i*) Our computational experience is that the computational cost of a progressive design is usually close to the one of a one-shot design, and more information is produced.
(*ii*) When using another initial controller, the asymptotic value of α should remain the same, since the whole set of stabilizing controllers is obtained whatever the initial stabilizing controller. Nevertheless, the minimal size of the basis for $Q(s)$, necessary to achieve the asymptotic value, depends on the initial controller. The more satisfactory the initial controller, the simpler the design of the Youla parameter to obtain the asymptotic achievable performance.
(*iii*) It would also be possible to introduce H_2 constraints or minimization objectives on $M_1(s)$ and $M_2(s)$.

Figure 2.4 presents the trade-off between the gain G, which more or less represents actuator activity, and the minimized value of α. The same basis (3.2) of $Q(s)$ is used, as well as the same initial H_∞ controller. G belongs to the set 1, 3, 5, . . . , 15, noting that the constraint seems infeasible for $G = 1$. As expected, the lower the allowed actuator activity, the harder the constraint, the higher the minimized objective.

One now details how the frequency domain cutting plane solver of section 2.2.3 works for $\omega_0 = 20\ rad/s$ and $G = 5$. A one-shot design is performed, i.e. all 64 filters are introduced at the same time. Remember the design frequency gridding is iteratively refined by adding worst-case frequencies, computed by validating the

optimized Youla parameter on a fine frequency gridding. Here is a sketch of the result:

```
 Minimisation objective between  2.868 and  2.918 (1.702e-002 percent)
Spec. 1 violated: max. value of the normalised objective =  6.862 greater than 2.947 at w = 13.567 rad/s
Spec. 2 violated: max. value of the normalised objective =  5.250 greater than 2.947 at w = 14.620 rad/s
Spec. 3 violated: max. relative violation of the template =  1.674 at w = 1000.000 rad/s

 Minimisation objective between  3.022 and  3.024 (5.914e-004 percent)
Spec. 1 violated: max. value of the normalised objective =  4.279 greater than  3.054 at w =  8.720 rad/s
Spec. 2 violated: max. value of the normalised objective =  4.885 greater than  3.054 at w = 12.689 rad/s
Spec. 3 violated: max. relative violation of the template =  1.053 at w =  8.704 rad/s
(...)
 Minimisation objective between  3.157 and  3.307 (4.537e-002 percent)
Relative tolerance, with which the frequency domain templates must be satisfied = 1.000e-002
Spec. 1 OK    : max. value of the normalised objective =  3.307 less than  3.340 at w =  8.080 rad/s
Spec. 2 OK    : max. value of the normalised objective =  3.239 less than  3.340 at w = 12.790 rad/s
Spec. 3 OK     : max. relative value w.r.t. the template =  1.007 at w = 12.316 rad/s

 alfa˙opt = 3.307e+000
```

A first minimization is performed with the initial design frequency gridding. When validating the Youla parameter on the fine frequency gridding, all 3 specifications, i.e. the 2 H_∞ minimization objectives and the H_∞ constraint, appear largely violated. A second minimization is performed: logically, the minimized objective increases since the problem is more constrained, due to the larger size of the design frequency gridding. At the end all 3 specifications are satisfied, up to a given specified numerical tolerance, namely 1 % here.

For a given design frequency gridding, here is an example of result of the cutting plane solver:

```
 SEARCH OF A FEASIBLE POINT

    1: constrmax = 4.201e+000 (64 variables)
(...)
   28: constrmax = 1.666e+000 (64 variables)
   29: constrmax = 6.138e-001 (64 variables)

 MINIMISATION OF THE OBJECTIVE

     1: gamma between 2.899e+000 and 6.783e+001 (64 variables)
(...)
    51: gamma between 3.022e+000 and 3.296e+000 (64 variables)
```

52: gamma between 3.022e+000 and 3.024e+000 (64 variables)

Minimisation objective between 3.022 and 3.024 (5.914e-004 percent)

First, a feasible point is looked for, which satisfies the constraints (the normalized constraint "*constrmax*" above should be less than unity). Next, lover and upper bounds of the minimized objective "*gamma*" are computed, until the gap becomes small enough.

As a last point, it is worth emphasizing that subgradients are kept from an optimization to an other in all the above examples:

1. When iteratively refining the design frequency gridding, for a given number of filters.
2. When progressively introducing the filters.
3. When studying the trade-offs.

This enables to save a large amount of computational time.

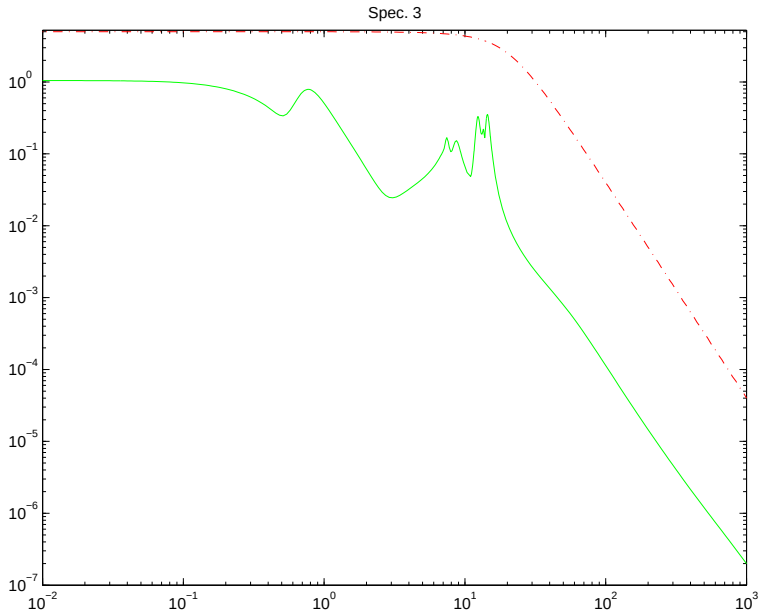

Figure 3.5: Closed loop frequency response $\overline{\sigma}(M_3(j\omega))$ without the Youla parameter.

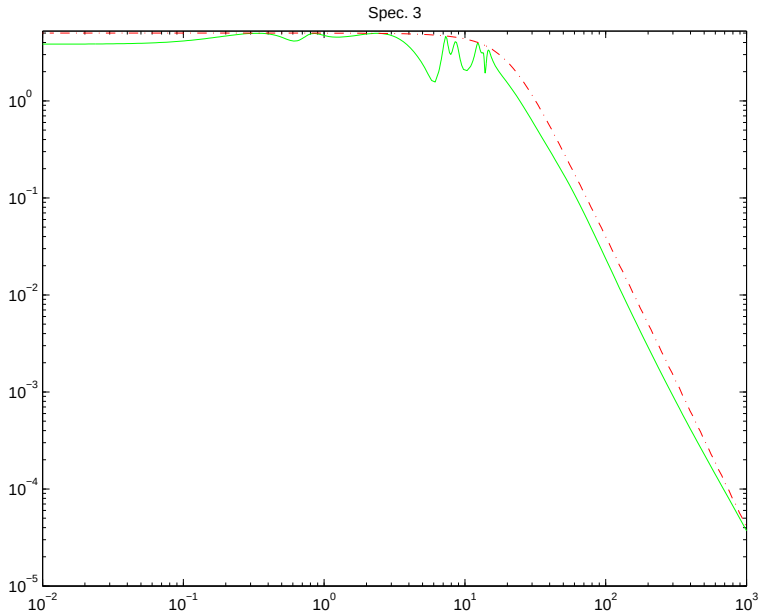

Figure 3.6: Closed loop frequency response $\overline{\sigma}(M_3(j\omega))$ with the Youla parameter.

Chapter 4

Convex design of a Youla parameter for an LFT plant model

4.1 Introduction to gain-scheduled control

To a large extent, gain-scheduling techniques [13, 20] can be divided into two main categories, depending on the design specifications. These can correspond to the frozen-time linearizations, or to the I/O behaviour of the nonlinear plant. The best known example of this second type of gain-scheduling approach is the LPV one. The nonlinear model is put under an LPV form, typically a polytopic or an LFT one, and the scheduling parameters are supposed to be time-varying, without or with a bound on their rate of variation, see e.g. [18, 23]. A closed-loop L_2 gain is usually minimized. It is worth emphasizing that the obtained (quasi-) LPV model is supposed to represent the I/O behaviour of the "true" nonlinear system, or at least to encompass it, so that constraining the L_2 gain of the closed loop LPV model also constrains the L_2 gain of the "true" closed loop nonlinear model.

As for the gain-scheduling techniques that handle frozen-time linearizations, the most classical one designs LTI controllers at several trim points of a nonlinear plant, and interpolate them a posteriori. Some techniques exist to guarantee a posteriori the closed loop stability and performance between the points of gridding [22], noting that their practical implementation appears difficult on challenging high order examples, e.g. a flexible aircraft. Another method which handles frozen-time linearizations is the Robust Modal Control technique, extended to the gain-scheduled and LFT cases [15, 16]. The scheduling parameters are supposed to be time-invariant, which is consistent with the fact that the time invariant linearizations correspond to the trim points of a nonlinear plant.

In the same way, as an extension of the work in [6], the aim of this chapter is to directly synthesize an LPV/LFT controller which satisfies modal and H_∞ design specifications on a continuum of time invariant linearizations. The main advantage

of the technique is its capability to handle several modal and I/O specifications (nearly) without conservatism, even within the context of LTI scheduling parameters. Moreover, the controller can easily be retuned at a finite set of trim points, which can be a key issue from an industrial point of view.

Last note that the results presented in this chapter could be considered as reminiscent of the work in [14]. Nevertheless, [14] deals with the case of a discrete-time LFT model with arbitrarily time-varying parameters, while this chapter deals with a continuous-time LFT model with LTI parameters. Moreover, [14] does not propose a controller design approach, unlike this chapter.

4.2 Problem statement

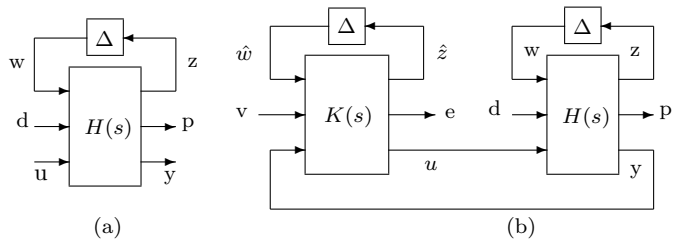

Figure 4.1: Open loop LFT model (a) and Youla parameterization for the gain-scheduled case (b).

On figure 4.1.a, the continuum of open loop linearizations is described as an LFT model

$$\begin{bmatrix} p \\ y \end{bmatrix} = F_u(H(s), \Delta) \begin{bmatrix} d \\ u \end{bmatrix},$$

where the structured model perturbation $\Delta = diag(\delta_k I_{q_k})$ contains the normalized scheduling parameters δ_k (repeated q_k times on the diagonal). Let $\delta = (\delta_k)_{k\in[1,\, n]}$ be the corresponding vector. Δ belongs to the unit ball $B\Delta$ (i.e. $\overline{\sigma}(\Delta) \leq 1$) if and only if δ belongs to the unit hypercube D (i.e. $\delta_k \in [-1,\ 1]\ \forall k$). Let a state-space representation of the augmented open loop plant model $H(s)$ be

$$\dot{x} = Ax + B_1 w + B_2 d + B_3 u \tag{4.1}$$
$$z = C_1 x + D_{11} w + D_{12} d + D_{13} u \tag{4.2}$$
$$p = C_2 x + D_{21} w + D_{22} d + D_{23} u \tag{4.3}$$
$$y = C_3 x + D_{31} w + D_{32} d + D_{33} u. \tag{4.4}$$

u and y denote the physical I/O used by feedback, d is an unmeasured disturbance and p an output relevant of performance. Δ is introduced as the fictitious feedback

$w = \Delta z$. For the ease of notation $D_{33} = 0$ is assumed in the following. The issue is twofold:

1. Compute an observed state-feedback LFT controller by computing gain-scheduled state-feedback and observer gains $K(\delta)$ and $L(\delta)$. The open loop LFT model is embedded inside the observer. The poles of this initial closed loop are requested to have a minimal damping ratio ξ and a minimal degree of stability $\lambda > 0$, $\forall \delta \in D$.

2. This initial closed loop is modified so as to compute a Youla parameterization of stabilizing controllers: the closed loop transfer matrix between d and p can be written under the affine form $T_1(s,\delta) + T_2(s,\delta)Q(s,\delta)T_3(s,\delta)$ w.r.t. the Youla parameter $Q(s,\delta)$. The closed loop transfer matrices $T_i(s,\delta)$, which correspond to the initial closed loop, are fixed. The design parameter $Q(s,\delta)$ is computed so as to satisfy H_∞ specifications $\forall \delta \in D$.

The state-feedback gain $K(\delta)$ is chosen under the form

$$K(\delta) = \sum_{j=1}^{L} p_j(\delta) K_j, \tag{4.5}$$

where the multivariate polynomial or rational functions $p_j(\delta)$, with values in $\Re$, are fixed while the matrices K_j are free. The same applies to the observer gain $L(\delta)$. The key point is to handle an affine representation of $K(\delta)$ or $L(\delta)$ as a function of the design parameters. Analogously, let

$$Q(s,\delta) = \sum_{j=1}^{M} q_j(\delta)\ Q_j(s),$$

where the free transfer matrices $Q_j(s)$ are put under the form

$$Q_j(s) = \sum_k \theta_{k,j} \mathcal{Q}_k(s)$$

The $\mathcal{Q}_k(s)$ are fixed while the $\theta_{k,j}$ are the design parameters. With an appropriate choice of the filters $\mathcal{Q}_k(s)$ [1], an orthonormal basis of filters is obtained.

4.3 Youla parameterization: the LFT case

Δ is supposed to be measured. A Youla parameterization is computed on the basis of a gain-scheduled observed state-feedback LFT controller. To this aim the following Lemma, whose proof is tedious but straightforward, proposes a closed loop structure described on figure 4.1.b. Below, to alleviate the notation, the state feedback and observer gains K and L are chosen not to depend on δ.

Lemma 4.1 *Let (4.1, 4.2, 4.3, 4.4) be a state-space representation of the augmented open loop plant model $H(s)$, with $D_{33} = 0$ and d an unmeasured disturbance input. Let an observed state feedback structure for the LFT controller be*

$$\begin{aligned} \dot{\hat{x}} &= A\hat{x} + B_1\hat{w} + B_3u + L\,e \\ \hat{z} &= C_1\hat{x} + D_{11}\hat{w} + D_{13}u \\ u &= -K\hat{x} + v \\ e &= y - C_3\hat{x} - D_{31}\hat{w}. \end{aligned} \tag{4.6}$$

The Youla parameter is introduced as $v = Q(s,\delta)e$. K and L are the state feedback and observer gains. Let $\delta x = x - \hat{x}$, $w = \Delta z$ and $\hat{w} = \Delta\hat{z}$. The closed loop state-space representation is

$$\begin{pmatrix} \dot{x} \\ \dot{\delta x} \end{pmatrix} = \mathcal{A}\begin{pmatrix} x \\ \delta x \end{pmatrix} + \begin{pmatrix} B_3 + B_1X_\Delta D_{13} \\ 0 \end{pmatrix} v + \begin{pmatrix} B_2 + B_1X_\Delta D_{12} \\ B_2 - LD_{32} + (B_1 - LD_{31})X_\Delta D_{12} \end{pmatrix} d$$

$$e = \begin{pmatrix} 0 & C_3 + D_{31}X_\Delta C_1 \end{pmatrix}\begin{pmatrix} x \\ \delta x \end{pmatrix} + (D_{32} + D_{31}X_\Delta D_{12})\,d,$$

with $X_\Delta = \Delta(I - D_{11}\Delta)^{-1}$ and

$$\mathcal{A} = \begin{pmatrix} A + B_1X_\Delta C_1 - (B_3 + B_1X_\Delta D_{13})K & (B_3 + B_1X_\Delta D_{13})K \\ 0 & A + B_1X_\Delta C_1 - L(C_3 + D_{31}X_\Delta C_1) \end{pmatrix} \tag{4.7}$$

Remark: $det(I - D_{11}\Delta) \neq 0$ is supposed for all $\Delta \in B\Delta$, as a classical well-posedness assumption of the open loop LFT plant model. Thus, X_Δ is well defined $\forall\Delta \in B\Delta$.

First note the triangular structure of the state-matrix $\mathcal{A}$ in equation (4.7). The separation principle is valid, i.e. it is possible to independently design the state-feedback and observer gains K and L, so as to place the closed loop poles in regions of the complex plane: see section 4.4.

Assume that d, $x(0)$ and $\hat{x}(0)$ are zero. A non-zero signal v induces a non-zero state vector x, but δx and e stay identically zero. Thus, the transfer matrix between v and e is zero. More precisely, on figure 4.1.b, the transfer matrix $T(s,\delta)$ between the inputs d and v and the outputs p and e has the structure:

$$T(s) = \begin{pmatrix} T_1(s,\delta) & T_2(s,\delta) \\ T_3(s,\delta) & 0 \end{pmatrix}$$

When choosing $v = Q(s,\delta)e$, the closed loop transfer matrix $T_1(s,\delta) + T_2(s,\delta)Q(s,\delta)T_3(s,\delta)$ between d and p is an affine function of the Youla parameter $Q(s,\delta)$. Moreover, the closed loop poles are those of the initial closed loop and those of the Youla parameter.

4.4 LTI Design of an observed state-feedback LFT controller

The issue is to design the state feedback and observer gains $K(\delta)$ and $L(\delta)$, so that the eigenvalues of (see equation (4.7))

$$\begin{aligned} A_{sf}(\delta, K(\delta)) &= A + B_1 X_\Delta C_1 - (B_3 + B_1 X_\Delta D_{13}) K(\delta) \\ A_{obs}(\delta, L(\delta)) &= A + B_1 X_\Delta C_1 - L(\delta)(C_3 + D_{31} X_\Delta C_1) \end{aligned}$$

have a minimal damping ratio ξ and a minimal degree of stability $\lambda > 0$, for all $\delta \in D$. In the following, one focuses on the design of a state feedback gain $K(\delta)$ under the form (4.5). The functions $p_j(\delta)$ are fixed, while the matrices K_j are the design parameters. The design principle is to combine a multi-model design step (1st subsection) with a validation step on the continuum (2d subsection).

4.4.1 Polytopic design of state-feedback and observer gains

Let $(A_i, B_i, C_i, 0)$ be a state-space representation of the strictly proper open loop plant $\#i$, with $i = 1, \ldots, N$. The issue is to design state feedback and observer gains K and L, so that the eigenvalues of $A_i - B_i K$ and $A_i - L C_i$ have a minimal damping ratio $\xi = cos(\alpha)$ and a minimal degree of stability $\lambda > 0$ for all $i = 1, \ldots, N$, with the additional difficulty that K and L depend on the scheduling parameters. Just the case of a state feedback gain is considered here, the technique is similar for an observer gain since the eigenvalues of $A_i - L C_i$ are also those of $A_i^T - C_i^T L^T$, which has the same structure as $A_i - B_i K$. Proposition 4.2 is an extension of [7] to the case of a gain-scheduled state-feedback gain. Its proof follows the one in this reference.

Proposition 4.2 *Let $(\delta^i)_{i \in [1,\ N]}$ be a finite set of values of the vector δ. Let $A_i = A + B_1 X_{\Delta^i} C_1$ and $B_i = B_3 + B_1 X_{\Delta^i} D_{13}$, where Δ^i is the value of the structured model perturbation Δ associated to δ^i. Thus $A_{sf}(\delta^i, K(\delta^i)) = A_i - B_i K(\delta^i)$, where $K(\delta)$ is defined in (4.5). If there exist one Lyapunov matrix $X = X^T > 0$ and matrices $W_j = K_j X$, with $j = 1, \ldots, L$, satisfying the LMIs $\forall i \in [1,\ N]$*

$$\begin{aligned} L_i + L_i^T + 2\lambda X &< 0 \\ \begin{pmatrix} sin\alpha \left(L_i + L_i^T\right) & -cos\alpha \left(L_i - L_i^T\right) \\ \star & sin\alpha \left(L_i + L_i^T\right) \end{pmatrix} &< 0, \end{aligned}$$

where

$$\begin{aligned} L_i &= L_i(X, W_1, \ldots, W_L) = (A_i - B_i \sum_{j=1}^{L} p_j(\delta^i) K_j) X \\ &= A_i X - B_i \sum_{j=1}^{L} p_j(\delta^i) W_j \end{aligned}$$

and $\star$ denotes the conjugate part of the hermitian matrix, then there exists a state feedback law $K(\delta)$ under the form (4.5), such that the eigenvalues of $A_i - B_i K(\delta^i)$ have a minimal damping ratio $\xi = cos(\alpha)$ and a minimal degree of stability $\lambda > 0$, with $K_j = W_j X^{-1}$.

4.4.2 Validation on the continuum with μ analysis

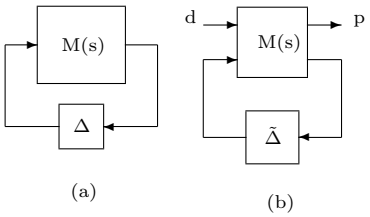

Figure 4.2: Standard interconnection structures for robust stability (a) and performance analysis (b).

Given the gain-scheduled state-feedback gain $K(\delta)$ designed in the preceding subsection, it must be checked if the eigenvalues of $A_{sf}(\delta, K(\delta))$ are inside the region $\mathcal{R}$, defined by a minimal damping ratio ξ and a minimal degree of stability $\lambda > 0$, for all $\delta \in D$. To be able to use μ tools, the key issue is to transform this problem into the robust stability analysis of the standard interconnection structure $M(s)$ - Δ of figure 4.2.a [8]. The nominal closed loop poles corresponding to $\Delta = 0$, i.e. the poles of $M(s)$, are assumed to strictly belong to $\mathcal{R}$. Then, it is tested if the poles of the interconnection structure still lie in $\mathcal{R}$ for all $\Delta \in B\Delta$, where Δ is supposed to be LTI. This reduces to the test $\mu(M(s)) \leq 1 \ \ \forall s \in \delta\mathcal{R}$, where $\delta\mathcal{R}$ denotes the border of $\mathcal{R}$ and the structured singular value μ is defined as follows.

Definition 4.3 *Let M be a given complex matrix and Δ be a structured model perturbation. $\frac{1}{\mu(M)}$ is defined as the $\overline{\sigma}$ norm of the minimal size model perturbation Δ that satisfies $det(I - \Delta M) = 0$.*

In practice, μ lower and upper bounds are computed instead of the exact value [8]. The next two Propositions explain how to validate the gain-scheduled state-feedback and observer gains $K(\delta)$ and $L(\delta)$ with μ analysis. Note that a preliminary requirement is to put $K(\delta)$ (and $L(\delta)$) under the standard LFT form $K_{11} + K_{12}\Delta_K(I - K_{22}\Delta_K)^{-1}K_{21}$, where $\Delta_K = diag(\delta_k I_{r_k})$. This is easily done using e.g. the LFR Toolbox [16]. The polynomial or rational functions $p_j(\delta)$ should be chosen to be well defined for all $\delta \in D$, so that it can be guaranteed that $det(I - K_{22}\Delta_K) \neq 0 \ \forall \Delta_K \in B\Delta_K$.

Proposition 4.4 *let* $A_{sf}(\Delta, K(\Delta_K)) = A + B_1 X_\Delta C_1 - (B_3 + B_1 X_\Delta D_{13}) K(\Delta_K)$, *with* $X_\Delta = \Delta(I - D_{11}\Delta)^{-1}$ *and* $K(\Delta_K) = K_{11} + K_{12}\Delta_K(I - K_{22}\Delta_K)^{-1}K_{21}$. *The state-feedback gain* $K(\Delta_K)$ *and the open loop plant model are supposed to be well-posed, i.e.* $det(I - K_{22}\Delta_K) \neq 0 \ \ \forall \Delta_K \in B\Delta_K$ *and* $det(I - D_{11}\Delta) \neq 0 \ \ \forall \Delta \in B\Delta$. *Then, let* $\mathcal{R}$ *be a given region of the complex plane, and assume that the nominal closed loop poles are strictly inside* $\mathcal{R}$, *i.e. the eigenvalues of* $A_{sf}(0, K(0))$. *The eigenvalues of* $A_{sf}(\Delta, K(\Delta_K))$ *stay inside* $\mathcal{R}$ *for all* $\Delta \in B\Delta$ *and* $\Delta_K \in B\Delta_K$ *if and only if*

$$det\left(I - M(s)\begin{pmatrix}\Delta & 0\\ 0 & \Delta_K\end{pmatrix}\right) \neq 0$$

for all $\Delta \in B\Delta$, *all* $\Delta_K \in B\Delta_K$ *and all* s *on the border* $\delta\mathcal{R}$ *of the region. A state-space representation of* $M(s)$ *is*

$$M(s) = \left(\begin{array}{c|cc} A - B_3K_{11} & B_1 & -B_3K_{12} \\ \hline C_1 - D_{13}K_{11} & D_{11} & -D_{13}K_{12} \\ K_{21} & 0 & K_{22} \end{array}\right)$$

Proposition 4.5 *let* $A_{obs}(\Delta, L(\Delta_L)) = A + B_1 X_\Delta C_1 - L(\Delta_L)(C_3 + D_{31} X_\Delta C_1)$, *with* $X_\Delta = \Delta(I - D_{11}\Delta)^{-1}$ *and* $L(\Delta_L) = L_{11} + L_{12}\Delta_L(I - L_{22}\Delta_L)^{-1}L_{21}$. *The observer gain* $L(\Delta_L)$ *and the open loop plant model are supposed to be well-posed, i.e.* $det(I - L_{22}\Delta_L) \neq 0 \ \ \forall \Delta_L \in B\Delta_L$ *and* $det(I - D_{11}\Delta) \neq 0 \ \ \forall \Delta \in B\Delta$. *Then, let* $\mathcal{R}$ *be a given region of the complex plane, and assume that the nominal closed loop poles are strictly inside* $\mathcal{R}$, *i.e. the eigenvalues of* $A_{obs}(0, L(0))$. *The eigenvalues of* $A_{obs}(\Delta, L(\Delta_L))$ *stay inside* $\mathcal{R}$ *for all* $\Delta \in B\Delta$ *and* $\Delta_L \in B\Delta_L$ *if and only if*

$$det\left(I - M(s)\begin{pmatrix}\Delta & 0\\ 0 & \Delta_L\end{pmatrix}\right) \neq 0$$

for all $\Delta \in B\Delta$, *all* $\Delta_L \in B\Delta_L$ *and all* s *on the border* $\delta\mathcal{R}$ *of the region. A state-space representation of* $M(s)$ *is*

$$M(s) = \left(\begin{array}{c|cc} A - L_{11}C_3 & B_1 - L_{11}D_{31} & L_{12} \\ \hline C_1 & D_{11} & 0 \\ -L_{21}C_3 & -L_{21}D_{31} & L_{22} \end{array}\right)$$

4.5 LTI design of the Youla parameter

The first subsection shows that the computation of a gain-scheduled Youla parameter $Q(s, \delta)$ reduces to the computation of an augmented Youla parameter $\mathcal{Q}(s)$, independent of δ. Thus, only the design of a fixed, i.e. non-gain-scheduled, Youla parameter $Q(s)$ is presented in the second subsection. The third explains how to combine multi-model design and validation on the continuum into a one-shot or iterative algorithm.

4.5.1 Case of a gain-scheduled Youla parameter $Q(s,\delta)$

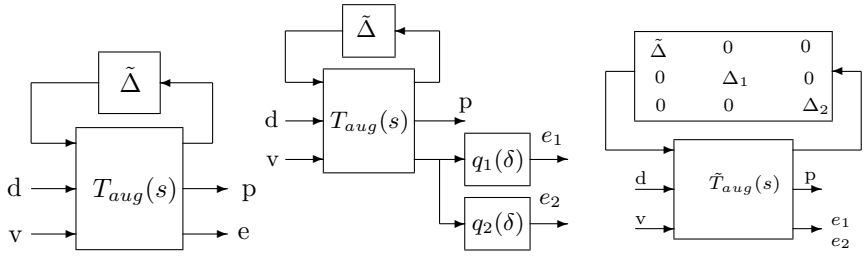

Figure 4.3: Interconnection structures for the design and validation of a gain-scheduled Youla parameter.

Consider the closed loop of figure 4.1.b, and rewrite it under the form of figure 4.3.a with $\tilde{\Delta} = diag(\Delta, \Delta)$. Remember that after connecting $v = Q(s,\delta)e$, the transfer matrix between d and p can be written under the form $T_1(s,\delta) + T_2(s,\delta)Q(s,\delta)T_3(s,\delta)$. If e.g. $Q(s,\delta) = q_1(\delta)Q_1(s) + q_2(\delta)Q_2(s)$, the functions $q_i(\delta)$ can be incorporated into figure 4.3.a, see figure 4.3.b. We have

$$\begin{aligned} v &= \mathcal{Q}(s)\begin{pmatrix} e_1 \\ e_2 \end{pmatrix} = \begin{pmatrix} Q_1(s) & Q_2(s) \end{pmatrix}\begin{pmatrix} e_1 \\ e_2 \end{pmatrix} \\ &= (q_1(\delta)Q_1(s) + q_2(\delta)Q_2(s))\, e \end{aligned}$$

Hence, the new design parameter is the unstructured asymptotically stable dynamic transfer matrix $\mathcal{Q}(s)$. Moreover, the static gains $q_i(\delta)$ can be put under an LFT form, so that the interconnection of figure 4.3.b can be put under the standard LFT form of figure 4.3.c, where Δ_i is the model perturbation associated to the LFT form of $q_i(\delta)$. The LFR Toolbox [16] can be helpful.

4.5.2 Design of a Youla parameter $Q(s)$

For the sake of clarity, one focuses on the simplified problem of computing the minimized worst-case H_∞ objective

$$J^* = \min_{Q(s)\in\mathcal{Q}} \max_{\delta\in D} \max_{\omega\in[0,\,+\infty)} \overline{\sigma}\left(T_1(j\omega,\delta) + T_2(j\omega,\delta)Q(j\omega)T_3(j\omega,\delta)\right). \tag{4.8}$$

$\mathcal{Q}$ is the space spanned by a finite N-dimensional orthonormal basis of filters $\mathcal{Q}_k(s)$, i.e. $Q(s) = \sum_{k=1}^{N} \theta_k \mathcal{Q}_k(s)$ where the θ_k are the optimization parameters while the $\mathcal{Q}_k(s)$ are fixed.

It is worth emphasizing that computing J^* is an infinite dimensional optimization problem, because of the double continuum of frequencies and parameters. The problem is convex despite the highly non-linear (LFT) structure of

$T_1(s,\delta) + T_2(s,\delta)Q(s)T_3(s,\delta)$. Indeed, let

$$J(Q(s)) = \max_{\delta\in D} \max_{\omega\in[0,\,+\infty)} \overline{\sigma}\left(T_1(j\omega,\delta) + T_2(j\omega,\delta)Q(j\omega)T_3(j\omega,\delta)\right). \tag{4.9}$$

Let $Q_1(s)$ and $Q_2(s)$ be two values of the Youla parameter. It is straightforward to prove that

$$J\left(\lambda Q_1(s) + (1-\lambda)Q_2(s)\right) \leq \lambda J(Q_1(s)) + (1-\lambda)J(Q_2(s))$$

In the same way as for the observed state-feedback LFT controller, the principle of the design technique on the continuum is to combine a multi-model design technique with a μ validation technique on the continuum. An interval of J^* is obtained.

A lower bound of J^* can be computed as

$$\underline{J} = \min_{Q(s)\in\mathcal{Q}} \max_{i\in[1,\,n]} \max_{\omega\in[0,\,+\infty)} \overline{\sigma}\left(T_1(j\omega,\delta^i) + T_2(j\omega,\delta^i)Q(j\omega)T_3(j\omega,\delta^i)\right), \tag{4.10}$$

where $(\delta^i)_{i\in[1,\,n]}$ is a set of values for the vector δ of scheduling parameters. In practice, this multi-model design problem can be solved either using a trivial extension of the state-space solution [21, 24] (one design model is considered in these references), or using the frequency-domain cutting planes method of section 2.2.

An upper bound of J^* can be obtained by computing (4.9) for a fixed value of $Q(s)$, typically the solution of (4.10). To this aim, connect $v = Q(s)e$ on figure 4.3.a, so that the transfer matrix between d and p becomes $F_l(M(s),\tilde{\Delta})$ on figure 4.2.b. At a given frequency ω, computing (4.9) reduces to computing the robust performance level

$$\gamma_{wc}(\omega) = \max_{\tilde{\Delta}\in B\tilde{\Delta}} \overline{\sigma}\left(F_l(M(j\omega),\tilde{\Delta})\right).$$

This standard robust performance problem reduces to a skew μ problem, see [8, 10] for details, i.e. skew μ lower and upper bounds are computed to obtain an interval of $\gamma_{wc}(\omega)$. An upper bound of $\gamma_{wc}(\omega)$ is a guaranteed (but potentially conservative) robust performance level, while the lower bound measures the accuracy of the upper bound. Moreover, a worst-value of $\tilde{\Delta}$ (and thus of the uncertain parameters δ_i) is provided with this lower bound.

When computing an upper bound of $\gamma_{wc}(\omega)$ over $\omega \in [0,\ +\infty)$ an upper bound of (4.9) is obtained, which is also an upper bound of J^*.

4.5.3 A one-shot or an iterative algorithm

Concerning the design over a model continuum of either the Youla parameter, or the observed state feedback LFT controller, several algorithms can be proposed.

The most general one is fully iterative: the controller, designed with a multi-model approach, is validated on the continuum. If the spec. are satisfied STOP, otherwise compute a worst-case model and add it to the set of design models...

A potentially faster and less cumbersome solution is one-shot: if there are few scheduling parameters the controller is designed e.g. on the vertices of the hypercube, and it is checked if the spec are satisfied on the continuum, so as to (in)validate the initial guess that the worst-case models are on the vertices.

More generally, on the basis of section 4.5.2, an algorithm can be developed to solve the generic problem of simultaneously minimizing several H_∞ control objectives under several H_∞ constraints over the continuum. As for the validation of the H_∞ constraints on the continuum a μ test can be performed, which is computationally less involved than a skew μ calculation. Moreover, if a convex H_∞ constraint reveals unfeasible during the multi-model design step, it is unfeasible on the continuum.

4.6 Conclusion

First, an extension of Youla parameterization to the case of gain-scheduled LFT controllers was proposed. On this basis, the Convex Control Design technique was extended to the case of an open loop LFT plant model. A technique was presented for the design of the initial observed state feedback LFT controller: using the separation principle the state feedback and observer gains are synthesized to satisfy pole placement inside an LMI region of the complex plane for the continuum of time invariant linearized closed loops. Next, the Youla parameter is designed to satisfy H_∞ specifications inside this continuum, by combining a convex multi-model design technique with a validation on the continuum using μ analysis.

An alternative for designing an LFT controller would be the use of classical μ synthesis techniques, but these non-convex schemes would just provide a local minimum. On the contrary, concerning at least the design of the Youla parameter, an infinite-dimensional convex optimization problem over a continuum of models is to be solved in our technique, due to the specific gain-scheduled closed loop structure. If the exact value of μ were computed the design problem could be exactly solved. The use of μ bounds complexifies the algorithm, but the gap between these bounds is usually small so that the design problem is expected to be nearly exactly solved. As an illustration, when minimizing a design objective over the continuum an (accurate) interval is obtained for the minimized value. This would not be possible using a non-convex optimization solver.

Chapter 5

A missile application

The technique of chapter 4 is applied to a non-linear missile example whose numerical data is extracted from [19]. The 4th order missile model contains a scalar input for feedback and two outputs α (angle of attack) and q (pitch rate), with a 2d order aerodynamic model (whose state vector is $[q, \alpha]$) and a 2d order actuator model (whose state vector is $[\eta,\ \dot{\eta}]$, where η is the actuator position and $\dot{\eta}$ is the actuator rate).

The open loop missile LFT model, which describes the continuum of time-invariant linearizations corresponding to trim points, is extracted from [8, 16], where $\Delta = diag(\delta_1 I_4,\ \delta_2 I_6)$ contains variations of α and the Mach number Ma. $\delta_i \in [-1,\ 1]$ corresponds to the validity domain of the nonlinear missile model, i.e. α between 0 and 20 degrees and Ma between 2 and 4.

As a preliminary, the well-posedness of this LFT model is checked by computing an upper bound of $\mu_\Delta(D_{11})$, see section 4.3. This μ upper bound is far below unity, which means that the open loop missile LFT model is well-posed largely beyond its validity domain.

5.1 Design of the initial observed state-feedback LFT controller

The state-feedback and observer gains can be chosen as constant, i.e. δ-independent. Noting that the observed state-feedback controller stays under an LFT form, since the open loop missile LFT model is embedded inside. When using the polytopic technique of section 4.4.1, the truncated sector is chosen as $\lambda = 1$ and $\xi = 0.6$. The state-feedback or observer gain is validated with the μ technique of section 4.4.2.

5.1.1 Multi-model design of the state feedback gain

The state feedback gain is synthesized first. An integrator is added on the output α. The design models are chosen as the 4 vertices of an enlarged square in the space of $(\delta_1,\ \delta_2)$, namely:

delta1 = +1.15, delta2= +1.15
delta1 = +1.15, delta2= -1.15
delta1 = -1.15, delta2= +1.15
delta1 = -1.15, delta2= -1.15

A constraint on the maximal magnitude of the poles is added in the polytopic LMI design of the state feedback gain, i.e. the magnitude of the closed loop poles must be less than r. This tuning parameter enables to modify the norm of the state feedback gain, as illustrated now. Very simply, r is automatically chosen using a dichotomy search, i.e. the minimal value of r is computed so that the LMIs are still feasible. This appears to minimize the norm of the state-feedback gain, as seen below:

r	vs	K
Inf		5057.6
1000.0		193.4
500.0		136.8
492.2		135.3
488.3		133.0

When checking the closed loop poles on the 4 design models, it is worth noting that the minimal value of the stability degree over the 4 models is 1.07, and the minimal damping ratio is 0.615, to be compared with $\lambda = 1$ and $\xi = 0.6$. This is due to the conservatism of the LMI polytopic technique, which stays (very) satisfactory at least in this case.

5.1.2 Validation of the state feedback gain on the continuum

The routine *mu_margin.m* of the Skew Mu Toolbox [10] is used to check that the closed loop poles stay inside the truncated sector defined by $\lambda = 1$ and $\xi = 0.6$ for all δ inside the unit square, i.e. inside the flight domain of validity of the missile model. To this aim a μ test can be performed, i.e. the issue is to check if the maximal μ upper bound over frequency is less than 1, which is found to be the case. A computationally more involved solution is to compute the maximal μ upper bound over frequency, obtained as:

mu upper bound = 0.883 at 17.367 rad/s

See figure 5.1 for an estimate of the μ upper bound as a function of frequency. The bars on this figure mean that μ is guaranteed to be less than β_i on the frequency interval $[\omega_i,\ \omega_{i+1}]$ [8], i.e. a peak on the μ plot cannot be missed, unlike what may happen when classically computing a μ upper bound on a frequency gridding.

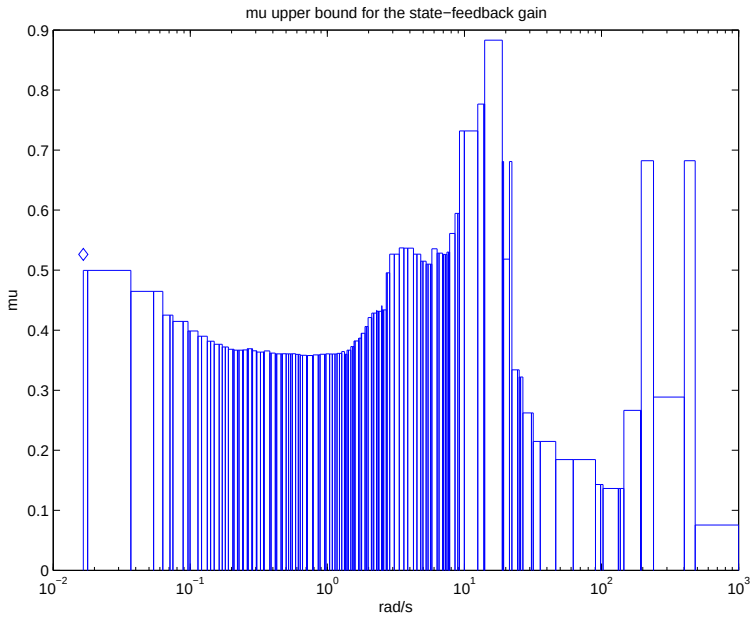

Figure 5.1: μ upper bound for the validation of the state-feedback gain on the continuum.

5.1.3 Multi-model design and validation of the observer gain

The observer gain is synthesized. Note that no integrator on the output α needs to be introduced in the observer model, since the state associated to the integrator is available. The design models are chosen as the 4 vertices of the *unit* square in the space of $(\delta_1,\ \delta_2)$. A constraint on the maximal magnitude r of the closed loop poles is introduced in the polytopic LMI design of the observer gain, so as to tune the norm of this gain, but this needs to be done manually. $r = 200$ is chosen.

When checking the closed loop poles on the 4 design models, the minimal value of the stability degree over the 4 models is 2.75, and the minimal damping ratio is 0.7, to be compared with $\lambda = 1$ and $\xi = 0.6$. The LMI polytopic technique is very conservative in this case.

When computing the maximal μ upper bound over frequency, one obtains:

mu upper bound = 0.805 at 0.000 rad/s

Since this upper bound is less than unity, the closed loop poles are guaranteed to stay in the truncated sector defined by $\lambda = 1$ and $\xi = 0.6$, inside the flight domain of validity of the missile model.

5.2 Computation of the Youla parameterization

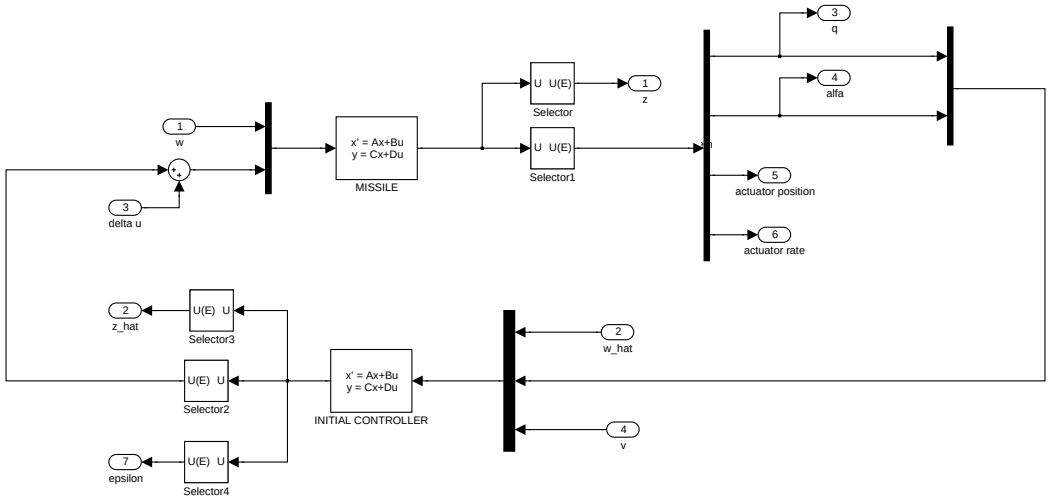

Figure 5.2: Simulink file describing the closed loop LFT model.

The Youla parameterization is computed with the Simulink file of figure 5.2. The first and second blocks of I/O (labeled w, w_hat, z and z_hat) correspond to the interconnection of the open loop plant model and initial controller with the Δ blocks (i.e. $w = \Delta z$ and $\hat{w} = \Delta\hat{z}$). The third input (labeled *delta u*) is an unmeasured additive disturbance δu on the feedback input. The 4th input (labeled v) is used to connect the Youla parameter $Q(s)$, i.e. $v = Q(s)e$ where the observation error e is output # 7 (labeled *epsilon*). Outputs # 3 to 6 are q, α, the actuator position η and the actuator rate $\dot{\eta}$.

Remark: a more efficient implementation could use the LFR-Simulink tools.

5.3 Design of the Youla parameter

5.3.1 Design specifications

The two design specifications, to be satisfied on the continuum of models, are the following. Let $H_1(s, \delta)$ (resp. $H_2(s, \delta)$) be the closed loop transfer function between

δu and the output α (resp. $\dot{\eta}$). Let

$$\mathcal{H}_i = \max_{\delta \in D} \max_{\omega} |H_i(j\omega, \delta)|.$$

The issue is to minimize $\mathcal{H}_1$ under the constraint $\mathcal{H}_2 \leq C$. C will take on several values in the following. Thus, the issue is to minimize the effect of an unmeasured disturbance on the angle of attack (which is the most relevant output for performance), under a constraint on the actuator activity.

5.3.2 Analysis of the initial controller

An interval is computed for the values of $\mathcal{H}_1$ and $\mathcal{H}_2$ when $Q(s) = 0$. To this aim, instead of computing skew μ bounds [8, 10], a simpler solution is chosen with a lower computational burden.

A lower bound $\underline{\mathcal{H}}_i$ of $\mathcal{H}_i$ is calculated by simply computing $|H_i(j\omega, \delta)|$ over the frequency ω for a gridding of 25 values of δ over the unit square. An upper bound is computed by testing $\mathcal{H}_i \leq \lambda$ over the continuum for several values of λ. A good initial guess is $\lambda = 1.2\underline{\mathcal{H}}_i$, i.e. the lower bound is assumed to be accurate. Testing $\mathcal{H}_i \leq \lambda$ reduces to a μ test over frequency, for which an efficient frequency sweeping technique is available [8, 10].

For the initial controller, this method gives:

spec. 1: w.c. perf. level between 0.660 and 0.693 (gap = 4.729 percent)
spec. 2: w.c. perf. level between 1.029 and 1.065 (gap = 3.315 percent)

which means that $\mathcal{H}_1 \in [0.660,\ 0.693]$ and $\mathcal{H}_2 \in [1.029\ C_0,\ 1.065\ C_0]$, where the normalizing factor is $C_0 = 150$. Note the good accuracy of the results, i.e. the gap between the bounds is low for both $\mathcal{H}_1$ and $\mathcal{H}_2$.

5.3.3 One-shot solution

A one-shot multi-model design of $Q(s)$ is performed, where the design models are simply the 4 vertices of the square. The poles of the basis of $Q(s)$ are simply chosen as the same pole -20 repeated 6 times (Laguerre basis).

First consider $C = C_0 = 150$. The following result is obtained:

spec. 1: w.c. perf. level between 0.193 and 0.208 (gap = 6.882 percent)
spec. 2: w.c. perf. level between 0.993 and 1.034 (gap = 3.899 percent)
guaranteed value of the w.c. minimization objective = 0.208

For the optimal value of $Q(s)$, whose order is 6, one obtains $\mathcal{H}_1 \in [0.193,\ 0.208]$ and $\mathcal{H}_2 \in [0.993\ C,\ 1.034\ C]$, with $C = 150$. The guaranteed value of the minimization

objective has been largely reduced, from 0.693 to 0.208. The constraint is satisfied with a reasonable tolerance.

Next consider $C = 170$. The following result is obtained:

spec. 1: w.c. perf. level between 0.120 and 0.129 (gap = 7.208 percent)
spec. 2: w.c. perf. level between 0.991 and 1.027 (gap = 3.560 percent)
guaranteed value of the w.c. minimization objective = 0.129

This means that $\mathcal{H}_1 \in [0.120,\ 0.129]$ and $\mathcal{H}_2 \in [0.991\ C,\ 1.027\ C]$, with $C = 170$. The result appears very sensitive to the value of C, since the guaranteed value of the minimization objective is 0.129 for $C = 170$, instead of 0.208 for $C = 150$. This illustrates the capability of the convex design technique to explore tradeoffs between specifications.

5.3.4 Iterative solution

The design is now iteratively performed on a gridding of 25 models over the unit hypercube. This means that at the end of the design, before validating the result on the continuum, the specifications should be satisfied on all 25 models. But inside the design process, worst-case models are iteratively determined, so as to avoid designing the Youla parameter on all 25 models. To this aim, the following algorithm is used:

1. Choice of the first initial worst-case model (the first of the gridding in the following, as an arbitrary choice).
2. Design of the Youla parameter on the current list of worst-case models.
3. Validation on the whole gridding of models. If the specifications are satisfied on all the gridding, STOP. Otherwise, determine the model for which the specifications are the most violated and insert it into the list of worst-case models. Go back to step 2.

Let $C = 150$. Only 3 worst-case models are needed to design a Youla parameter which minimizes $\mathcal{H}_1$ under the constraint $\mathcal{H}_2 \leq C$ over the gridding of 25 models. Then, the result is validated on the continuum:

spec. 1: w.c. perf. level between 0.186 and 0.213 (gap = 12.634 percent)
spec. 2: w.c. perf. level between 1.003 and 1.045 (gap = 4.001 percent)
guaranteed value of the w.c. minimization objective = 0.213

The result is consistent with the one obtained using a one-shot solution.

Chapter 6

Conclusion

A Youla-parameterization technique was presented, for transforming a feedback design problem into a convex optimization problem, where the minimization objective and constraints directly correspond to time- and frequency-domain design specifications. The case of an LTI model was considered first, before extending the method to the LFT case. A frequency-domain cutting planes solver was developed, which is especially suited for the case of high order models. The technique was applied to an LTI, rather high order, flexible aircraft model and to an LFT missile model. The ability to explore the necessary trade-offs between the design specifications was illustrated, as well as the interest of using a dedicated solver: keeping subgradients from one optimization to another enables to save a large amount of computational time.

EMPTY PAGE

Bibliography

[1] H. Akcay and B. Ninness.
Orthonormal basis functions for continuous-time systems and Lp convergence.
Mathematics of Control, Signals and Systems, 12(3):295–305, 1999.

[2] D. Alazard and P. Apkarian.
Observer-based structures of arbitrary compensators.
International Journal of Robust and Nonlinear Control, 9(2):101–118, february 1999.

[3] B.D.O. Anderson.
From Youla-Kucera to identification, adaptive and nonlinear control.
Automatica, 34(12):1485–1506, 1998.

[4] D.J. Bender and R.A. Fowell.
Computing the estimator-controller form of a compensator.
International Journal of Control, 41(6):1565–1575, 1985.

[5] D.J. Bender and R.A. Fowell.
Some considerations for estimator-based compensator design.
International Journal of Control, 41(6), 1985.

[6] S.P. Boyd and C.H. Barratt.
Linear Controller Design. Limits of Performance.
Prentice Hall, 1991.

[7] M. Chilali and P. Gahinet.
H_∞ design with pole placement constraints: an LMI approach.
IEEE Transactions on Automatic Control, 41(3):358–367, 1996.

[8] G. Ferreres.
A practical approach to robustness analysis with aeronautical applications.
Springer Verlag, 1999.

[9] G. Ferreres and P. Antoinette.
Convex gain-scheduled control of an LFT model.
Proc. of the ECC, 2009.

[10] G. Ferreres and J.M. Biannic.

A Skew Mu Toolbox (SMT) for robustness analysis.
available on the authors' homepages, 2003-2009.

[11] G. Ferreres and G. Puyou.
Flight control law design for a flexible aircraft: limits of performance.
Journal of Guidance, Control and Dynamics, 29(4):870–878, July-August 2006.

[12] R.A. Hyde and K. Glover.
The application of scheduled H_∞ controllers to a VSTOL aircraft.
IEEE Transactions on Automatic Control, 38(7):1021–1039, 1993.

[13] D.J. Leith and W.E. Leithead.
Survey of gain scheduling analysis and design.
International Journal of Control, 73(11):1001–1025, 2000.

[14] W.M. Lu, K. Zhou, and J.C. Doyle.
Stabilization of uncertain linear systems: an LFT approach.
IEEE Transactions on Automatic Control, 41(1):50–65, 1996.

[15] J.F. Magni.
Robust Modal Control with a Toolbox for use with MATLAB.
Springer Verlag, April 2002.

[16] J.F. Magni.
Linear Fractional Representation Toolbox.
Available on the author's homepage, 2004-2008.

[17] D. McFarlane and K. Glover.
Robust controller design using normalized coprime factor plant descriptions.
Lecture Notes in Control and Information Sciences. Springer Verlag, 1990.

[18] A. Packard.
Gain scheduling via linear fractional transformations.
Systems and Control Letters, 22:79–92, 1994.

[19] R.T. Reichert.
Dynamic scheduling of modern robust control autopilot design for missiles.
IEEE Control System Magazine, 12(5):35–42, October 1992.

[20] W.J. Rugh and J.S. Schamma.
Research on gain scheduling.
Automatica, 36:1401–1425, 2000.

[21] C.W. Scherer.
An efficient solution to multi-objective control problems with LMI objectives.
Systems and Control Letters, 40:43–57, 2000.

[22] D.J. Stilwell and W.J. Rugh.
Interpolation of observer state feedback controllers for gain scheduling.
IEEE Transactions on Automatic Control, 44(6):1225–1229, 1999.

[23] F. Wu, X.H. Yang, A. Packard, and G. Becker.
Induced L_2 norm control for LPV systems with bounded parameter variation rates.
International Journal of Robust and Nonlinear Control, 6:983–998, 1996.

[24] M.J. Zandvliet, C.W. Scherer, C.W.J. Hol, and M.M.J. van de Wal.
Multi-objective H_∞ control applied to a wafer stage model.
Proceedings of the IEEE CDC, pages 796–802, 2004.

EMPTY PAGE